RTD-TDR-63-4012

RESEARCH IN BOUNDARY LAYER OSCILLATIONS AND NOISE

TECHNICAL DOCUMENTARY REPORT RTD-TDR-63-4012

FEBRUARY 1964

AF FLIGHT DYNAMICS LABORATORY
RESEARCH AND TECHNOLOGY DIVISION
AIR FORCE SYSTEMS COMMAND
WRIGHT-PATTERSON AIR FORCE BASE, OHIO

Project No. 1370, Task No. 137005

(Prepared under Contract No. AF 61(052)-358 by
University of Southampton, Hampshire, England;
M. K. Bull and J. L. Willis, authors)

NOTICES

When Government drawings, specifications, or other data are used for any purpose other than in connection with a definitely related Government procurement operation, the United States Government thereby incurs no responsibility nor any obligation whatsoever; and the fact that the Government may have formulated, furnished, or in any way supplied the said drawings, specifications, or other data, is not to be regarded by implication or otherwise as in any manner licensing the holder or any other person or corporation, or conveying any rights or permission to manufacture, use, or sell any patented invention that may in any way be related thereto.

Qualified requesters may obtain copies of this report from the Defense Documentation Center (DDC), (formerly ASTIA), Cameron Station, Bldg. 5, 5010 Duke Street, Alexandria 4, Virginia

This report has been released to the Office of Technical Services, U.S. Department of Commerce, Washington 25, D.C., in stock quantities for sale to the general public.

Copies of this report should not be returned to the Aeronautical Systems Division unless return is required by security considerations, contractual obligations, or notice on a specific document.

300 - March 1964 - 162-29-568

FOREWORD

The research work in this report was performed by the University of Southampton, Hampshire, England, for the Aero Acoustics Branch, Vehicle Dynamics Division, AF Flight Dynamics Laboratory, Wright-Patterson Air Force Base, Ohio under Contract Nr AF 61(052)-358. This research is part of a continuing effort to obtain data and techniques for defining important vibration and acoustic phenomena in flight vehicles which is part of the Research and Technology Division, Air Force Systems Command's exploratory development program. The Department of Defense Program Element number is 6.24.05.36.4, "Space Flight Dynamics". This work was performed under Project Nr 1370, "Dynamic Problems in Flight Vehicles" and Task Nr 137005, "Methods of Noise Prediction, Control, and Measurement". Mr. D. I. Smith and later Mr. P. H. Hermes of the AF Flight Dynamics Laboratory were the project engineers.

This work was administered by the Office of Aerospace Research, USAF through its European Office in Brussels, Belgium. Assistance was provided by Major O. J. Manci, Jr. and Capt. R. C. Coupland, Jr. of the EOAR.

ABSTRACT

Experimental data are presented on the r.m.s. levels, frequency spectra, probability distributions and space-time correlations of the pressure field as a whole, and in narrow frequency bands, for turbulent layers on smooth surfaces. General qualitative effect of a surface discontinuity on the r.m.s. pressure and frequency spectrum are given. An empirical representation of the space-time correlation pattern of the pressure field is developed for the purposes of structural response calculations. A general program for the study of a mechanism of boundary layer turbulence is presented along with a discussion of the testing and analyzing instrumentation. An analytical method is presented for the prediction of the power spectral density of panel response to boundary layer and siren excitation. An empirical equation is developed relating the acoustic power output from a unit area of a (large) surface subject to turbulent boundary layer flow to the aerodynamic flow parameters.

This report has been reviewed and is approved.

Howard A. Magrath

HOWARD A. MAGRATH
Chief, Vehicle Dynamics Division
AF Flight Dynamics Laboratory

LIST OF CONTENTS

LIST OF ILLUSTRATIONS

LIST OF SYMBOLS

a	speed of sound
A	panel area
A_r, B_n	coefficients in the empirical representation of surface pressure correlation
f	frequency, cps
G	fraction of time signal exceeds arbitrary reference level
$J_{N_{rr}}(f)$	joint acceptance for pressure field and panel mode
k	wave number
K	characteristic wave number of fluctuating pressure field
m	mass per unit area of panel
M_r	generalized mass associated with mode r
$N_{mhs}(\frac{\omega}{u}, \delta)$	Fourier transform of space correlation with respect to coordinate in flow direction = $N_{mhs}(k, \delta)$
p	fluctuating surface pressure
p'	rms surface pressure fluctuations = $\sqrt{\langle p^2 \rangle}$
$P(\xi, \delta, \tau)$	pressure correlation referred to a fixed coordinate system = $\langle p(x,y,t)\, p(x+\xi, y+\delta, t+\tau) \rangle$
$P_M(\xi, \delta, \tau)$	pressure correlation referred to convected coordinate system = $\langle p(x,y,t)\, p(x+\xi, y+\delta, t+\tau) \rangle_M$
$P_{M\xi\delta}(\xi, \delta)$	normalized space-pressure correlation referred to convected coordinate system = $P_M(\xi, \delta, 0)/\langle p^2 \rangle$
$P_{M\tau}(\tau)$	normalized time-pressure correlation referred to convected coordinate system = $P_M(0, 0, \tau)/\langle p^2 \rangle$

$\tilde{P}_f(\xi,\delta,\tau)$	normalized excitation pressure cross-power spectral density
q	dynamic pressure = $\frac{1}{2}\rho U^2$
S	surface area
$S(\omega)$	power spectral density of fluctuating pressure
t	time
U	fluid velocity
U_c	convection velocity
W	acoustic power
Y	arbitrary reference level for intermittency measurements
Y_r	panel impedance for mode r
α	characteristic frequency of the pressure fluctuations
γ	intermittency value
δ^*	displacement thickness of the boundary layer
δ	length increment in y-direction
θ	measure of the lifetime of the turbulence element
μ	"hysteretic" damping coefficient
ξ	length increment in x-direction
ρ	fluid density
τ	time increment
τ_0	wall shear stress
$\Psi_r(R)$	shape of the panel mode of order r
$\Psi_r(s)$	mode shape evaluated at point s
$\Phi_{ww}(f)$	displacement power spectral density
$\Phi_p(f)$	excitation pressure power spectral density
$\Phi_p(f;\underline{\xi},\underline{\xi}';\tau)$	excitation pressure cross-power spectral density

1. Introduction

This report is intended to summarize the work carried out under Contract No. AF 61(052)-358 over the period March 1960 to March 1962.

Results which have already been included in Contract Technical Notes are briefly summarized with mention of any additional results since obtained. This applies mainly to the characteristics of the turbulent boundary layer pressure field. Other topics which have not been fully reported on previously, such as the measurements planned for the laminar-turbulent transition region and the calculation of response of panels to turbulent boundary layer excitation are treated in a little more detail.

Data have been obtained on the r.m.s. levels, frequency spectra, probability distributions and space-time correlations of the pressure field as a whole, and in narrow frequency bands, for turbulent boundary layers on smooth surfaces, and some effects of surface discontinuities have also been investigated. The work has reached a stage where the statistical characteristics of the wall pressure field of a turbulent boundary layer can be fairly accurately defined in terms of the flow parameters, certainly sufficiently well to provide a realistic representation of the excitation of a panel or structure subjected to this field. Empirical formulae representing the pressure field have been derived for this purpose, and have also been used to obtain a figure for the level of radiated sound which would result from turbulent flow over a rigid boundary surface.

The study of the wall pressure fluctuations is now being extended to the region where transition from laminar to turbulent flow occurs: development of the measuring apparatus is now sufficiently well advanced to allow

Manuscript released by the authors in June 1963 for publication as an RTD Technical Documentary Report.

experimental work to proceed and preliminary results are included in this report.

The calculation of panel response to random loading has been programmed for a digital computer. Estimates of the response of a $3\frac{1}{2}$" square test panel to turbulent boundary layer excitation have been made and similar calculations are now being made to obtain the response of the same panel to various forms of excitation in the siren tunnel. Measurements of panel response are proceeding in parallel with this work.

Experiments to measure the levels of sound transmitted by structural vibrating resulting from flow excitation have been planned to follow panel response measurements.

2. Wall Pressure Field Associated with Boundary Layer Flow

2.1 Pressure Field of a Fully-Turbulent Boundary Layer

2.1.1 Flow Facilities and Instrumentation for Fluctuating Pressure Measurements

2.1.1.1 Flow Facilities

Early measurements were made on the turbulent boundary layers on the walls of the 6" x $2\frac{1}{2}$" wind tunnel[1] and the vertical 2" water tunnel[2] At the present time measurements are being made in the 9" x 6" wind tunnel which is very similar in construction to the 6" x $2\frac{1}{2}$" tunnel.

2.1.1.2 Pressure Transducers

Various forms of pressure transducer using piezoelectric discs of lead zirconate-titanate ceramic as sensitive element have been developed, with crystal diameters ranging from 0.030" to 0.170". The construction and

shock-tube calibration of these instruments has been described previously[1][2].

Transducers using two crystals and electrical adding circuits as a method of cancelling unwanted vibration pick-up have been built. The performance of one of these is referred to in Section 2.2.3.

2.1.2 Statistical Properties of the Wall Pressure Field

2.1.2.1 R.M.S. Pressure

Measured values of r.m.s. pressure have been related to surface friction and extrapolated to zero transducer size[2]. This resulted in a value of $p'/\tau_o = 2.5$ at low speeds. The effects of increasing flow Mach number seems to be to produce a slow increase in the value of p'/τ_o to about 3 at M = 1.5. Tests in the 9" x 6" wind tunnel should provide additional information on Mach Number effects.

2.1.2.2 Frequency Spectrum, Space-Time Correlations and Convection Speeds

The results of the experimental measurements of these quantities have been previously presented in Reference 2, where empirical representations of the data were also given. The power spectrum of the pressure fluctuations was obtained as

$$\frac{S(\omega)U_\infty}{q_\infty^2 \delta^*} = \left[5.32e^{-\left(\frac{\omega\delta^*/U_\infty}{1.125}\right)^2} - 1.25e^{-10\left(\frac{\omega\delta^*/U_\infty}{1.125}\right)^2}\right] \times 10^{-5} \qquad \ldots(2.1)$$

which is consistent with convection of a virtually frozen pressure pattern with a space correlation in the flow direction of

$$\frac{\langle p(x,z,t)p(x+\xi,z,t)\rangle}{\langle p^2\rangle} = 1.08e^{-10\left(\frac{\xi/\delta^*}{4.5}\right)^2} - 0.08e^{-\left(\frac{\xi/\delta^*}{4.5}\right)^2} \qquad \ldots(2.2)$$

The auto-correlation of the pressure field referred to axes moving at the convection speed was given as

$$P_{M\tau}(\tau) = 0.693e^{-200\left(\frac{\tau U_\infty/\delta^*}{200}\right)^2} + 0.180e^{-15\left(\frac{\tau U_\infty/\delta^*}{200}\right)^2} + 0.127e^{-\left(\frac{\tau U_\infty/\delta^*}{200}\right)^2} \quad \ldots(2.3)$$

Additional experimental work carried out since these relationships were first obtained has in general supported the numerical magnitudes chosen. The 2" water tunnel measurements showed a rate of decay of the pressure field considerably greater than was obtained in other work and represented by Equation (2.3). (See Fig. 24 of Reference 2). These measurements have been examined in some detail and corrections applied to the space-time correlation values for the effects of equipment noise and a low-level acoustic standing wave in the tunnel working section. The resulting values are in very close agreement with Equation (2.3).

In Reference 2 it was suggested that in view of the lack of information the form of the space-correlation in the lateral direction should be taken to be the same as that in the flow direction. Some preliminary measurements of the lateral correlations have been made in the 9" x 6" wind tunnel with a flow speed of about 500 ft/sec., but so far the minimum transducer separation which has been examined is about $5\delta^*$. At this spacing the correlation coefficient is very nearly zero and appears to be slightly negative. This indicates that the scale of the field in the lateral direction is not greatly different to the longitudinal scale.

The convection speed of the wall pressure pattern obtained from water tunnel measurements increased with separation of the measuring points from $0.7U_\infty$ at $\xi/\delta^* \sim 2$ to $0.85U_\infty$ at $\xi/\delta^* \sim 20$. A similar effect has now been observed in the 9" x 6" wind tunnel where the convection velocity appears to be in the region of $0.7U_\infty$ for $\xi/\delta^* \sim 5$ increasing to $0.8U_\infty$ at $\xi/\delta^* \sim 10$

and remaining constant at this value for separations up to 25 δ^*. The effect seems to indicate that the small scale components of the pressure field result from rapidly decaying small motions in the low mean velocity region of the boundary layer relatively close to the wall while the large scale components are associated with slowly decaying large scale motion in the outer region of the layer.

2.1.2.3 Probability Distribution

An examination of the pressure signals from the water tunnel boundary layer has shown that the amplitude distribution is very nearly Guassian[2].

2.1.2.4 Effects of Surface Irregularities

Results of measurements of r.m.s. pressures and frequency spectra in the region of step discontinuities in the wall of the 2" water tunnel have been reported in Reference 2. Generalization of the results is not possible, although some trends were indicated. For example the energy in the low frequency region of the spectrum increased progressively with the height of the discontinuity, but attempts to obtain a non-dimensional representation of the effect in terms of the height of the discontinuity were not successful.

A probability analysis of signals from the disturbed regions showed that the relative frequency of large amplitude excursions tended to increase as the measuring point approached the discontinuity.

Increase of r.m.s. pressure of up to twice the smooth wall value were observed.

2.1.3 Empirical Representation of the Wall Pressure Field

To provide a self-consistent representation of the space-time correlation pattern of pressure field for purposes of structural response calculations the following empirical representation based on the existing experimental data was suggested[2].

$$\frac{\langle p(x,z,t)p(x+\xi,z+\zeta,t+\tau)\rangle}{\langle p^2\rangle} = \frac{P(\xi,\zeta,\tau)}{\langle p^2\rangle} = \frac{P_M(\xi - U_c\tau,\zeta,\tau)}{\langle p^2\rangle}$$

$$\frac{P_M(\xi,\zeta,\tau)}{\langle p^2\rangle} = \frac{P_M(\xi,\zeta,0)}{\langle p^2\rangle}\,\frac{P_M(0,0,\tau)}{\langle p^2\rangle} \qquad \ldots(2.4)$$

$$= P_{M\xi\zeta}(\xi,\zeta).\ P_{M\tau}(\tau)$$

where $P_M(\xi,\zeta,\tau)$ is the space-time correlation of the pressure field in a frame of reference moving at the convection velocity U_c. The form of $P_{M\xi\zeta}(\xi,\zeta)$ and $P_{M\tau}(\tau)$ and the numerical values chosen were

$$P_{M\xi\zeta}(\xi,\zeta) = \sum_r A_r e^{-rK^2(\xi^2+\zeta^2)}$$

$$P_{M\tau}(\tau) = \sum_n B_n e^{-n\alpha^2\tau^2} \qquad \ldots(2.5)$$

with $K\delta^* = 1/4.5$

$r = 1 \quad A_1 = -0.08$

$r = 10 \quad A_{10} = 1.08$

$$\frac{\alpha\delta^*}{U_\infty} = \frac{1}{200} \qquad \ldots(2.6)$$

$n = 1 \quad B_1 = 0.127$

$n = 15 \quad B_{15} = 0.180$

$n = 200 \quad B_{200} = 0.693$

Equations (2.1) to (2.3) above are based on these relations.

2.1.4 Space-Time Correlation of Filtered Pressure Signals

For calculations of the response of a structure to boundary layer excitation using the normal mode approach, the space-time correlation of the pressure field in a narrow frequency band embracing the particular normal mode is required. In essence this information is contained in the overall correlations of the field and can be obtained by transformation, but it can also be measured directly. Measurements of correlation in frequency bands were made first by Harrison[4] but these results seemed to indicate a unique dependence of the correlation on $\omega\xi/U_c$. Such a relation leads to scale anomalies at low frequencies. Additional measurements were made in the 6" x 2½" wind tunnel[1] and the form of the results to be expected in the case of a slowly decaying pressure field as encountered in a slowly growing boundary layer was also investigated[3].

It was concluded in Reference 3 that

(1) the frequency band space-time correlation in the flow direction is periodic in time delay and spatial separation, undamped in time, but with spatial damping depending on spatial separation and convection velocity.

(2) the variation in correlation amplitude with spatial separation in the stream direction can be derived directly from the moving frame overall autocorrelation of the pressure field.

A variation of this form removes the scale anomaly at low frequencies and on the basis of the relations given in Equations (2.5) and (2.6) it was found that the correlation amplitude could be expected to fall from unity to 0.2 with spatial separating increasing from zero to about $36\,\delta^*$. The derived rate of spatial decay was found to be a tolerable representation of the measured frequency band correlations (Fig. 7 of Reference 3) at least for frequencies in the energy contained range of the spectrum.

2.2 Wall Pressure Fluctuations in the Laminar-Turbulent Transition Region

2.2.1 Aim of Experiments

The aim of these experiments is to continue the studies on the basic mechanism of boundary layer turbulence by investigating the properties of the turbulent processes found in the laminar-turbulent transition region, with particular reference to wall pressure fluctuations.

The transition region has been selected for study since it is here that the generation of turbulence first occurs in a field with known properties, namely, the laminar boundary layer. It is hoped, therefore, that some insight will be gained into the process of turbulence production, and hence ultimately, the mechanism by which the turbulent boundary layer is sustained.

To make these studies use is being made of a hot-wire/microphone combination. Selection of only those parts of the flow it is desired to study will be made by another hot-wire driving a specially designed piece of apparatus (see below). In this way, examination of turbulent spots at all stages of their development may be made.

There have been some delays in this programme due to the difficulty of setting up the instrumented transition region, and to the design and construction of the special equipment needed to study intermittent phenomena. These difficulties have been surmounted, and some preliminary results are presented.

2.2.2 Experimental Programme

As it is now understood, the process of transition from laminar to turbulent flow occurs gradually over a distance in the downstream direction due to the superposition of distinct turbulent patches or spots. These turbulent spots are believed to arise from the growth of small disturbances in the laminar boundary layer which at some crucial stage in their development form into a limited region of turbulence. This spot diffuses as it is

convected downstream by the mean flow until is loses its separate existence through its interaction with other spots.

Over this region, where both laminar and turbulent flow regimes are to be found, the degree of "spottiness" is described by the intermittency of the flow. The intermittency may be defined either as the fraction of time for which the flow is laminar (the "laminar intermittency", denoted here by G), or the fraction of time for which the flow is turbulent (the "turbulent intermittency", denoted by γ), As the latter is the one in general use in the literature, the term intermittency will hereafter be used for turbulent intermittency.

It is intended to study the turbulence in the spots in the transition region. In particular, it is hoped to study the pressure fluctuations associated with the transition region, the character of the turbulence in the spots, and the position in the layer where the turbulence appears first. This last aspect may be of importance in relation to the observed convection of the pressure field of a turbulent layer at 0.8 of the free stream velocity, since it has been suggested that this effect is due to phenomena near the surface excited in conditions in the outer part of the boundary layer.

Recent advances in knowledge of transition have been made by Schubauer, Klebanoff and others[5] using a vibrating ribbon to artificially induce transition. It is not planned at the moment to use this technique, but to study the statistical characteristics of the flow with natural transition.

The basic configuration for the instrumentation is shown in Fig. 11. Studies of the field will be made using a microphone and hot-wire (marked "active wire"), and the outputs from each will be analyzed both separately and also as a joint record by correlation techniques. In order that

the turbulence in the region of the microphone may be limited to newly developed spots, another hot-wire placed upstream of the microphone (marked "monitor wire" will be used to operate a device which will shut off the microphone signal if the turbulence is passing over the monitor wire. Although only one channel is treated in this way, the effect after correlation is as though both active hot-wire and microphone outputs were processed by the monitor wire.

2.2.3 Instrumentation of the Transition Region

In order to make a study of the transition region with acoustic instrumentation it is necessary to have some control over the position at which transition occurs, since the exact position is very sensitive to external flow conditions which vary from day to day, and it is not in general possible to move the microphones about readily. Basically, in a wind tunnel, the option is between a boundary layer on a surface specially mounted for that purpose, or using the tunnel wall.

At the time these measurements were first envisaged, the only low noise tunnel immediately available was an induced flow one with a working section measuring 6" x 2.5" which had been in use for turbulent boundary layer measurements. The speed in the working section of this tunnel was fixed at about 500 f.p.s. by a downstream sonic choke. As the flow had been stabilized by placing boundary layer trips at the entrance it was not possible to study transition on the working section walls, and so a plate was mounted in the working section for this purpose. The high frequencies characteristic of the flow, and the very limited space available, made the use of the piezo-electric crystal transducers previously used in this tunnel for pressure measurements imperative. It was not possible in the space to incorporate any form of mechanical vibration isolation for the crystal, so a vibration

cancelling technique was evolved using two crystals. The two crystals were mounted rigidly on the plate and one of them was screened from the pressure field; their electrical outputs were combined to cancel the acceleration effects. Unfortunately, the presence of the plate excited strong acoustic resonances in the tunnel, and as it would have required extensive modification to the tunnel to avoid them this arrangement was abandoned. The method of vibration compensation of the pressure transducers is of some interest, however, and the degree of success can be judged from Fig. 1, where the suppression of the plate modes is evident.

At this stage a new tunnel of a similar type to the one mentioned above, but with a working section measuring 9" x 6", was complete. It was thought that a suitable transition region could be established on the wall of this tunnel at the beginning of the working section, the position of transition being controlled by sucking away various amounts of the boundary layer. However, the flow tended to become turbulent upstream of the suction slots, so that satisfactory control of transition could not be obtained. It was not considered feasible with the conditions present to re-stabilize the boundary layer once it had become turbulent.

It was decided, therefore, to revert to study of the transition region on a flat plate, and to adapt a low speed tunnel specially for the work, replacing the existing entrance with a new inlet, working section and diffuser, and altering the fan gearing. The existing aluminium sheet diffuser was treated with "Aquaplas", and as much of the new structure as possible was made with acoustically inert fibre board. The resulting tunnel offers a speed of up to 100 f.p.s. in the working section. A diagram of the arrangement is shown in Fig. 2, and of the working section in Fig. 3.

The working surface is a $\frac{1}{4}$" brass plate, highly polished, with a flat

upper surface and a 6° wedge cut on the leading edge. A slight waviness is visible to the eye, but the surface is smooth to the touch. A small hole, diameter 0.030", is drilled 7" from the leading edge, giving access to a cavity for a ½" condenser microphone (Brüel and Kjaer type 4134) which is mounted on the underside of the plate, and recessed to within 0.029" of the top surface. Control of boundary layer transition is effected by adjusting the pressure gradient in the working section by means of flexible wall liners.

2.2.4 Turbulence Monitoring and Gating Equipment

Fundamental to the concept of these experiments is the ability of the instrumentation to distinguish between signals characteristic of laminar and turbulent flow. The way in which the apparatus for doing this function is described below.

The core of this apparatus is a detecting (or rectifying) system to which a variable bias may be applied. To illustrate the working, suppose for simplicity that the signal to be examined is a sine wave, as shown in Fig. 4 and we wish to know for what fraction of the period T the amplitude is above some arbitrary level, y. It will be seen that at time t_1 the amplitude becomes greater than y, and stays so until time t_2; the appropriate fraction is

$$G = (t_2 - t_1)/T = \tfrac{1}{2}\left[1 - \frac{\sin^{-1}y}{\pi}\right] \qquad \ldots(2.7)$$

since $t_1 = \sin^{-1}y$

$t_2 = \pi - \sin^{-1}y$

The output of an ideal device for a given setting, y, would be given

by Equation 2.7, and varies from G = 0 (level never above y for $y \geq 1$) to G = 0.5 (half wave rectification) for y = 0, when the apparatus is examining positive parts of the signal. In practice it is necessary that an increasing (decreasing) signal exceed (fall below) the setting y by some small amount before the apparatus can be made aware of it. Errors introduced by this effect are greatest at the peak. This and other similar effects due to finite operating times can, however, be reduced by careful design. Some idea of the magnitude of possible errors can be obtained from Table 1.

TABLE 1

Error due to Non-Ideal Operation of Trigger Circuit for Positive Going Portion of Sine Waves

Necessary excess in fraction of signal / y	0.2	0.4	0.6	0.8	0.95
0.01	0.003	0.004	0.005	0.009	0.018
0.05	0.007	0.008	0.010	0.018	0.035
0.10	0.033	0.038	0.049	0.088	0.175

Error given in fraction of whole period.

If this basic device is presented with an intermittent signal and the level y made just high enough not to be reached by the instrument noise (see Fig. 6), then the device will "fire" at the peaks, but there will be a dead zone around the axis, equal to 2y, in which it will shut off. To overcome this, it is necessary to build in a "memory" which holds the device on for long enough to ensure that there is no further critical peak to follow. The last super-critical peak will be followed then by a fallacious extension

to the time of the spot. This process is shown in Fig. 6,where the unmodified gating signal and signal with time delay are illustrated for a hypothetical input signal.

The circuit diagram is shown in Fig. 8, and block diagram for the circuit in Fig. 9. The signal input (marked "Monitor input") is amplified and passes to a signal inverter, which has a two-channel output, one being the same as the input signal and the other the input signal inverted. This is done so that both positive and negative portions of the signal can be examined, the detecting circuit being sensitive to positive going signals only. After further amplification each part of the signal passes to the detector system, which is,in essence, a diode to which a variable bias may be applied, thus passing the proportion of the signal above the critical (bias) level. The resulting clipped signal is amplified so that the input to the Schmitt Trigger has sharp rise characteristics. The Schmitt Trigger produces square pulses as wide as the clipped peaks remaining from the detector. These pulses pass to the Time Delay, which imparts an exponential decay to their trailing edges, the rate of decay being variable by simply altering the appropriate capacitances. The result is to effectively widen the pulses which are presented to the second Schmitt Trigger, the output of which is used to operate a gating circuit.

Any signal may be applied for gating ("Active input"), including the monitor signal itself. As arranged, the gate is <u>shut</u> when the critical levels are exceeded in the detector, and hence is normally open. Thus, the result of passing any intermittent signal through the gating system will be to remove those parts of it which occur at times when the monitor signal exceeds the critical level.

A counting system has also been provided for use with the circuit

for quantitative measurements of intermittency. In this case, the input to the gate is a 200 kcps sine wave. The output is passed through three binary counters, which reduce the effective frequency to 12.5 kcps, before operating a timed decade counter. In this way the fraction of the time for which the monitor signal is sub-critical is simply the ratio of the counts with and without monitor input.

The last mentioned facility provides an accurate means of assessing the accuracy of the device, since by varying the clip level in the detector it is possible to determine how much of the given signal is greater than a given amplitude - effectively a probability analyser. Thus for a sine wave, the fraction is given by Equation 2.7, while a similar evaluation may be made for white noise. The results of actual tests are shown in Figs. 5 and 7. It is seen that the operation of the equipment is satisfactory.

2.2.5 Results Obtained to Date

As this equipment was only made operational a short time before this writing it has not been possible to accumulate any extensive experimental results. However, some preliminary results have been taken, and are presented below.

2.2.5.1 Calibration

The initial calibration of the microphone showed a flat response to about 2000 c.p.s. after which acoustic resonances produced a rather peaky and generally rising response to about 10,000 c.p.s. The application of damping material in the form of steel wool in the probe bore has reduced the peaks, although the gradual rise is still present. All the same the response curve is flat to within $\pm$ 4 db up to 10 kcps., which is above the expected cut-off frequency for the spectrum of the turbulence given by the Strouhal number relation

$$f\delta^*/U_\infty \sim 0.1$$

leading to $f \sim 6000$ c.p.s. for $U_\infty = 100$ f.p.s.

$\delta^* = 0.020"$

The background noise, which is dominated by discrete fan frequencies at about 150 c.p.s. and (to a lesser extent) at 300 c.p.s., is at an acceptable level of about 94 db, although the low frequencies do show up in the correlation coefficient obtained from hot-wire and microphone signals, and will be eliminated by filtering when necessary. The free stream turbulence level, as measured with the new low-noise transistor hot-wire gear, is about 0.3% of the free stream mean velocity, and as this level does not seem to be having any adverse effect on the transition phenomenon, no attempt is being made to reduce it at present.

To examine different parts of the transition region, it is necessary to alter the pressure gradient slightly with the tunnel liners. While this gives the microphone effectively a variable x co-ordinate relative to the beginning of the transition region, it also has some effect on the length of the actual zone over which transition occurs. An estimate of the extent of the transition region is to be had if it is assumed that the plot of intermittency v. distance along the plate resembles an integrated Gaussian Error function. There is experimental support for this assumption. The intermittency measured at two points 4.2" apart was 0.138 and 0.778. For this case turbulence can be expected for 1% of the time 4.5" upstream of the leading station, and 90% at 3.5" downstream of the trailing station, although the assumption of Gaussian form is almost certainly in error at this distance. However, the extent of the region is probably of the order of about 9".

2.2.5.2 Intermittency Measurements

Fig. 12 shows intermittency measured at various stations in the boundary layer for two stations in the transition region, one where the layer is mainly laminar and the other where the layer is mainly turbulent. Though it is inevitable with such measurements that there should be relatively large scatter, both curves are quite well defined. It will be seen that there exists a marked variation in the measured intermittency across the boundary layer, maximum values being observed at about 0.15 δ and 0.65 δ, where δ is the thickness of the undisturbed laminar layer. If one part of the layer predominates in the production of turbulent spots, and it is assumed that the spots grow uniformly as they are convected downstream, it may be shown that the observed intermittency in this region will be higher than elsewhere. It is possible, therefore, that one or both of the maxima observed in Fig. 12 correspond to areas of turbulence production.

2.2.5.3 Pressure Measurements

Measurements have also been made of the pressure fluctuations, using a hot-wire placed immediately over the microphone to evaluate the intermittency. The hot-wire signal is to be preferred for this purpose to the microphone output as the signal/noise ratio is much better, but it has the disadvantage that (as can be seen from Fig. 12) the intermittency measured at a fixed distance from the surface will only approximately represent the value of the wall pressure intermittency; the value obtained in this way, however, can be expected to be fairly representative of the pressure intermittency. The microphone output was integrated over a period of 30 seconds and divided by this intermittency to arrive at a value for the r.m.s. wall pressure associated with the turbulent spots.

Measurements with full turbulence at a flow speed of 70 feet per

second gave a pressure level of 104 db re 0.0002 dyne/cm^2. For this measurement the microphone was calibrated against a standard noise source. This makes the ratio

$$p'/q = 9.5 \times 10^{-3}$$

where p' is the r.m.s. value of the pressure fluctuations, and q is the dynamic pressure, which is the same as that obtained by Harrison[4]. This preliminary figure is subject to revision, but indicates no significant difference from the fully developed turbulent boundary layer.

The pressure associated with the spots for different intermittencies (different effective downstream stations) is shown in Fig. 10, together with the accuracy limits. As the intermittency approaches zero, (fully laminar), both the integrated value of the pressure signal and the divisor (γ) become very small. If the error in the r.m.s. pressure P is p, and in the measured intermittency γ is g, then the quotient is

$$p' = \frac{P \pm p}{\gamma \pm g}$$

Since approximately $p = kP$

then $$p' = \frac{P}{\gamma} \frac{1 \pm kP/\gamma}{1 \pm q/\gamma} \approx \frac{P}{\gamma} \left(1 \pm \frac{kp}{\gamma} \mp \frac{g}{\gamma}\right)$$

p and g are fixed in any given situation so that the limit lines vary hyperbolically with γ . The limits are given for 2% error in P, and 3% in γ . Both are rather optimistic estimates, but it is seen that the resulting lines nearly enclose the pressure points from fully turbulent down to about 30% turbulent. Agreement is poorer at very low values where the error is of the order of the mean value. The mean value used in Fig. 10 may be made to coincide with the fully turbulent value (γ = 1.0) by using a different value of intermittency; as discussed in Section 2.2.5.2 above, the precise

intermittency which is applicable is still in doubt. Fig. 11 then indicates that the pressure field associated with the turbulent spots is similar to that of fully developed turbulence.

2.2.5.4 Continuation

Work is proceeding for the time being with the single wire and microphone combination discussed above. In particular, further work is being done on the variation of intermittency across the boundary layer, and on the variation of amplitude distribution, which has been observed to be markedly skew. It is proposed not to proceed with two wire work until the possibilities of the present configuration have been exploited; the necessary facilities for doing this are already available.

3. Theoretical Response of Panel to Turbulent Boundary Layer Excitation

3.1 Results to Date

The work done so far has been based on the results derived by Powell[6] for the response of structures to random excitations, and solutions are, therefore, obtained as the sum of solutions in each of a multitude of normal modes. The limitation of this approach is that response in each mode has to be derived separately, with the consequence that, in general, a large amount of computation is needed to get even an approximate evaluation of the panel displacements in quite a narrow frequency range.

As yet the range of frequencies covered is limited to the region 0 - 1000 c/s. which includes the first 15 panel modes.

3.2 Basis of Calculations

3.2.1 Equations used

Equation (13a) of Reference 6 for the power spectral density of panel displacement can be written in the form

$$\frac{\varpi_z(f)}{\varpi_p(f)} = \sum_r \frac{\psi_r^2(\underline{R})AI \; j^2_{Nrr}(f)}{|Y_r|^2} + \sum_r \sum_{s \neq} \frac{\psi_r(\underline{R})\psi_s(\underline{R}) \; AI \; j^2_{Nrs}(f)}{|Y_r||Y_s|} \qquad \ldots(3.1)$$

where

$$j^2_{Nrs}(f) = \frac{1}{\varpi_p(f) \; AI} \int_A \int_A \varpi_p(f;\underline{s},\underline{s}';\tau)\psi_r(\underline{s})\psi_s(\underline{s}')d^2\underline{s} \; d^2\underline{s}'$$

$$= \frac{1}{AI} \int_A \int_A \tilde{P}_f(\xi,\zeta,\tau)\psi_r(\underline{s})\psi_s(\underline{s}') \; d'\underline{s} \; d'\underline{s}' \qquad \ldots(3.2)$$

$$I = \int_A \psi_r^2(\underline{s}) \; d^2\underline{s} \; ; \; A = \text{Panel Area} \qquad \ldots(3.3)$$

Here $\varpi_z(f)$, $\varpi_p(f)$ are power spectral densities of panel displacement z at $\underline{R}$, and exciting pressure p respectively, at a frequency f c/s.

$\varpi_p(f;\underline{s},\underline{s}';\tau)$ is the cross-power spectral density of the excitation,

$\psi_r(\underline{s})$ is the mode shape considered evaluated at point $\underline{s}$.

$\tilde{P}_f(\xi,\zeta,\tau) = \tilde{P}_{\omega}(\xi,\zeta,\tau)$ is normalised cross-power spectral density of the excitation

$\omega = 2\pi f$

$= \left|\frac{\theta_r - \theta_s}{\omega}\right|$

$Y_r = |Y_r| e^{-i\theta r}$ is panel impedance for mode r.

3.2.2 Panel Impedance

The form used here is

$$|Y_r| = M_r \left\{ (\omega_r^2 - \omega^2)^2 + \mu^2 \omega_r^4 \right\}^{\frac{1}{2}} \qquad \ldots(3.4)$$

$$= M_r \omega_r^2 \left\{ \left[1 - \left(\frac{\omega}{\omega_r}\right)^2 \right]^2 + \mu^2 \right\}^{\frac{1}{2}}$$

$$\tan \theta_r = \frac{\mu}{1 - \left(\frac{\omega}{\omega_r}\right)^2} \qquad \ldots(3.5)$$

Here μ, a "hysteretic" damping coefficient, is taken as 0.005, but the actual value taken has little significance, except for frequencies near to the natural frequency for the mode considered, provided only that it is of the right order of magnitude.

3.2.3 Effect of Cross Terms

As stated in the Section 3.1 we are confining our activities for the moment to the low frequency range, so that it seems to be justifiable to assume that

$$\tau = \frac{|\theta_r - \theta_s|}{\omega}$$

will not be too close to zero, and, hence, that $\tilde{P}_f(\xi, \zeta, \tau)$ will be appreciably less than $\tilde{P}_f(\xi, \zeta, 0)$. This fact, combined with the fact that the integral of a product of modal functions over part of the panel area will usually be less than the integral of the square of either of the modal functions over the same area, leads us to assume that

$$j^2_{Nrs}(f) \ll j^2_{Nrr}(f) \qquad \ldots(3.6)$$

$$r \neq s$$

The validity of this assumption for the particular correlation

function assumed is one of the matters that is to be investigated later.

Equation (3.1) is thus used in the reduced form

$$\frac{\varpi_f(f)}{\varpi_p(f)} \doteq \frac{\psi_r^2(\underline{R})\, AI\; j^2_{Nrr}(f)}{|Y_r|^2} \qquad \ldots(3.7)$$

3.3 Correlation Function

3.3.1 General Form

In Reference 3 the following form for $\tilde{P}_f(\xi, \zeta, \tau)$ for a slowly decaying pressure pattern is derived:

$$\tilde{P}_f(\xi, \zeta, \tau) = \frac{N_{MR\zeta}\left(\frac{\omega}{U_c}, \zeta\right)}{N_{MR\zeta}\left(\frac{\omega}{U_c}, 0\right)} P_{M\tau}\left(\frac{\xi}{U_c}\right) \cos\omega\left(\tau - \frac{\xi}{U_c}\right) \qquad \ldots(3.8)$$

where $P_{M\tau}(\tau)$ is the autocorrelation function referred to axes moving with convection velocity U_c, whilst the term

$$\frac{N_{MR\zeta}\left(\frac{\omega}{U_c}, \zeta\right)}{N_{MR\zeta}\left(\frac{\omega}{U_c}, 0\right)}$$

is taken to be the same as the overall lateral space correlation $P_{M\xi\zeta}(0, \zeta)$. So (3.8) is taken as

$$\tilde{P}_f(\xi, \zeta, \tau) = P_{M\xi\zeta}(0, \zeta)\, P_{M\tau}\left(\frac{\xi}{U_c}\right) \cos\omega\left(\tau - \frac{\xi}{U_c}\right) \qquad \ldots(3.9)$$

(See Reference 3, Section 4 from which this is taken).

i.e. $\tilde{P}_f(\xi, \zeta, 0) = P_{LAT} \times P_{LONG}$. $\qquad \ldots(3.10)$

P_{LAT}, P_{LONG} are overall lateral space correlation and longitudinal space correlation in required narrow frequency bands respectively.

3.3.2 Assumed Form for Boundary Layer Tunnel Correlation Function

Because of its analytical simplicity, the form which has been assumed initially for $P_{M\tau}(\tau)$ is that taken by Dyer in Reference 7. However, the computer programme can be extended to include correlation functions such as that proposed in Reference 2.

$$P_{M\tau}(\tau) = e^{-|\tau|/\theta} \qquad \ldots(3.11)$$

where $\frac{\theta U_\infty}{\delta^*} = 30$

Here $U_\infty = 500$ ft/sec

$\delta^* = 0.1"$

so that $\theta = 0.5$ m.sec.

Thus we can take

$$P_{LONG} = P_{M\tau}\left(\frac{\xi}{U_c}\right) \cos \frac{\omega\xi}{U_c}$$

$$= \exp\left[-\frac{\delta_L}{2}\frac{\xi}{\xi_o}\right] \cos 2\pi\left[\tfrac{1}{4}\frac{\xi}{\xi_o}\right] \qquad \ldots(3.12)$$

ξ_o = separation in longitudinal direction for first zero of P_{LONG}

δ_L = log decrement based on first (negative) peak.

i.e. for $\xi = 2\xi_o$

Then $2\pi f \frac{\xi}{U_c} = 2\pi\left[\tfrac{1}{4}\frac{\xi}{\xi_o}\right]$

$$\xi_o = \frac{100}{f} \text{ ft.} \qquad \ldots(3.13)$$

$$= \frac{1200}{f} \text{ ins.}$$

$$\frac{\xi}{U_c\Theta} = \frac{\delta_L}{2}\,\frac{\xi}{\xi_o}$$

$$\delta_L = \frac{1000}{f} \qquad \ldots(3.14)$$

There is very little experimental information on the value of P_{LAT}. It will be assumed that

$$\zeta_o = 2.5\,\delta^* = 0.25 \text{ ins} \qquad \ldots(3.15)$$

and the maximum negative value is 0.05.

So we take

$$P_{LAT} = \exp\left[-\frac{\delta_T}{2}\,\frac{\xi}{\zeta_o}\right]\cos 2\pi\left[\frac{1}{4}\,\frac{\zeta}{\zeta_o}\right] \qquad \ldots(3.16)$$

where $$\delta_T = 3.0 \qquad \ldots(3.17)$$

Equations (3.12) - (3.17) inclusive substituted into (3.10) give the assumed form for the correlation function.

3.3.3 Assumed Form for the Correlation Function for the Siren Tunnel

Here we assume $P_{LAT} = 1$ ...(3.18)

(Reference 8 Figure 14),

and assuming that for a given frequency the effective part of the pressure field is a cosine wave propagating at the speed of sound, we get

$$\delta_L = 0 \qquad \ldots(3.19)$$

$$\xi_o = \frac{3300}{f} \text{ ins.} \qquad \ldots(3.20)$$

so that

$$\tilde{P}_f(\xi, \zeta, 0) = P_{LONG} \qquad \ldots(3.21)$$

with values given in Equations (3.19) and (3.20).

3.4 Evaluation of $j^2_{Nrr}(f)$

In Reference 9 a relationship is derived for $j^2_{Nrr}(f)$ as defined in Equation (3.2)*, for a correlation function of the form

$$\tilde{P}_f(\xi,\zeta,0) = e^{-a_L|\xi|} \cos b_L\xi \; e^{-a_T|\zeta|} \cos b_T\zeta \qquad \ldots(3.22)$$

with $\psi_r(\underline{s})$ taking the form

$$\psi_r(\underline{s}) \equiv \psi_{mn}(\underline{s}) = \sin \frac{m\pi x}{L_x} \sin \frac{n\pi y}{L_y} \qquad \ldots(3.23)$$

The mode shape assumed here is appropriate to having the panel edges simply supported but there are indications that the effect of the plate boundary conditions on the integrated value of $j^2_{Nrr}(f)$ is small for the fundamental mode, and gets progressively smaller as the order of the mode increases, so that the error introduced by the assumption is probably small.

Using relations similar to Equations (3.22) and (3.23), Reference 9 derives

$$J^2_N(f) = \frac{16\phi_L\phi_T}{(mn\pi^2)^2} \qquad \ldots(3.24)$$

where

$$\phi = \frac{1}{\Delta^2}\left\{p\left[1-(-1)^m e^{-aL}\cos bL\right] + 4q(-1)^m e^{-aL}\sin bL + \frac{mr\Delta}{2}\pi\right\} \qquad \ldots(3.25)$$

$$\Delta = \left[1+\left(\frac{aL}{m\pi}\right)^2 + \left(\frac{bL}{m\pi}\right)^2\right]^2 - 4\left(\frac{bL}{m\pi}\right)^2 \qquad \ldots(3.26)$$

*This definition, rather than that used by Powell, is used to eliminate the effects of any arbitrary coefficients arising in the choice of $\psi_r(\underline{s})$.

$$p = \left[1 + \left(\frac{aL}{m\pi}\right)^2 - \left(\frac{bL}{m\pi}\right)^2\right]^2 - 4\left(\frac{aL}{m\pi}\right)^2\left(\frac{bL}{m\pi}\right)^2 \quad \ldots(3.27)$$

$$q = \left(\frac{aL}{m\pi}\right)\left(\frac{bL}{m\pi}\right)\left[1 + \left(\frac{aL}{m\pi}\right)^2 - \left(\frac{bL}{m\pi}\right)^2\right] \quad \ldots(3.28)$$

$$r = \left(\frac{aL}{m\pi}\right)\left[1 + \left(\frac{aL}{m\pi}\right)^2 + \left(\frac{bL}{m\pi}\right)^2\right] \quad \ldots(3.29)$$

where all symbols except numerical constants are understood to have suffix α and where α = L, T.

$$m_L = m, \; m_T = n.$$

The correspondence between Equation (3.22) and Equation (3.12) and (3.16) is given by

$$b_L = \frac{\pi}{2\xi_o}, \quad b_T = \frac{\pi}{2\zeta_o} \quad \ldots(3.30)$$

$$a_L = \frac{\delta_L}{2\xi_o}, \quad a_T = \frac{\delta_T}{2\zeta_o} \quad \ldots(3.31)$$

3.5 Evaluation of $|Y_r|^2$

3.5.1

From Equation (3.5)

$$|Y_r|^2 = M_r^2 \omega_r^4 \left\{\left[1 - \left(\frac{\omega}{\omega_r}\right)^2\right]^2 + \mu^2\right\} \quad \ldots(3.32)$$

where $$M_r = \int_A m\psi_r^2(\underline{s})\, d^2\underline{s} = mI \quad \ldots(3.33)$$

m = mass/unit area of panel.

Thus the evaluation of $|Y_r|^2$ centres on the evaluation of the natural frequencies of the panel in each of the modes considered.

3.5.2 Evaluation of ω_r^2

The natural frequency of the panel is derived using the work reported in Reference 10. The actual boundary conditions (i.e. fixed or supported depending on the panel) are used here, as distinct from the assumption made for Equation (3.23).

3.6 Final Equation

We now have all that is required for the evaluation of $\Phi_z(f)$ since for Equation (3.8)

$$\frac{\Phi_z(f)}{\Phi_p(f)} = \sum_{m,n} \frac{\psi_{mn}^2(\underline{R})}{m^2 \omega_{mn}^4 \left\{\left[1 - \left(\frac{\omega}{\omega_{mn}}\right)^2\right]^2 + \mu^2\right\} I_{mn}} \frac{A}{} j^2_N(f) \qquad \ldots(3.34)$$

where $$I_{mn} = \int_A \psi^2_{mn}(\underline{s})\, d^2\underline{s} \qquad \ldots(3.35)$$

and the $\psi_{mn}(\underline{s})$, ω_{mn} are those dictated by the actual plate boundary condition.

3.7 Panel Results

The panel being evaluated at the moment is an 0.005" thick steel panel, 3.5" square, and the panel is fastened to a solid member in such a way that it is reasonable to take it as having fully fixed edges.

The process indicated above has been carried through for this panel, the lowest 15 modes having been considered for the response in the boundary layer tunnel, but only, so far, the lowest mode for the siren tunnel case.

The results of the computations are shown in Fig. 13.

4. Response of Panels to Boundary Layer Excitation (Experimental)

4.1

The study of structural response to turbulent boundary layer excitation is of interest in relation to two major engineering problems; one is the problem of noise in and around aircraft and submarines where a major contribution results from the action of the structure as a transducer in converting the hydrodynamic pressures in the boundary layer into acoustic pressures and the other is that prolonged excitation by the boundary layer may cause structural failure due to fatigue. In an investigation into either of these problems it is desirable to have a knowledge of the response of simpler elements of a structure, such as panels, to random excitation.

Panel response to boundary layer excitation has been studied theoretically by several authors using either panel normal modes or the concept of coincidence (i.e. frequency and wavelength matching between exciting force and panel response). However, up to date there has been little or no experimental verification of the accuracy of estimation provided by either of these approaches and hence it is the object of the current investigation to obtain data, by measuring the response of panels to boundary layer excitation in air, which might provide (a) justification for the calculation procedures and (b) a clearer insight into the mechanism of the response of a structure to this type of excitation. The problem is complex and the model structures studied initially must of necessity be simple in form so that they are amenable to calculation. For this reason the measurements are being made on panels of square or rectangular plan-form, having fixed edges and having no longitudinal or transverse stiffeners.

In order to interpret the measurements fully, the vibrational

characteristics of the specimens must be known. For this reason the frequencies and shapes of the normal modes of the panels are determined experimentally using discrete frequency excitation. To complete the investigation, the response of the panels under test is being calculated theoretically, as described in Section (3) above, for comparison with the experimental values.

4.2 Preliminary Measurements in the 6" x 2½" Wind Tunnel

The initial work on panel response to boundary layer noise excitation was carried out in the supersonic working section of the 6" x 2½" tunnel. It was intended to investigate possible coincidence effects at supersonic convection velocities of the boundary layer pressure field, with particular reference to the generation of Mach waves by supersonic flexural ripples in the panel. This study proved impracticable in this small scale flow and when Mr. D.J.M. Williams left the group, this work was discontinued in favour of the panel displacement measurements in the 9" x 6" tunnel.

The work did, however, highlight one of the major difficulties in these investigations, namely the construction of the panel. When using thin sheets of metal it is extremely difficult to obtain a panel which is flat and yet under zero or negligible tension. The panel was formed from a sheet of brass, 0.005" thick, attached to a 6" diameter plug, the shape of the vibrating panel being determined by a 3½" square hole cut through the centre of the plug. The first panel was stuck to the plug with epoxy resin but the adhesive failed during trial runs in the tunnel. Later panels were attached to the plug by clamping strips parallel to the edges of the square hole. This method presented difficulties in fixing the brass sheet at the corners of the cut-out and introduced unknown and probably non-uniform

tension in the panel.

4.3 Test in the 9" x 6" Wind Tunnel

The measurements in the 9" x 6" tunnel are concerned with the displacements of panels subjected to boundary layer excitation and hence are of a rather different nature to those discussed above. The panels being tested are similar to those used in the 6" x 2½" tunnel in that they are formed from a thin sheet of metal attached to a 6" diameter plug with the hole in the plug again determining the shape of the vibrating region. The panels currently being used are 3½" square and either 0.005" or 0.010" thick. The material used has, however, been changed from brass to steel, so that the panels can be excited magnetically for determination of their normal modes of vibration.

Because of the possibility of introducing unknown tensions in the panels, and hence creating unpredictable effects in their response[6] the clamping procedure adopted in the earlier tests was not continued. Instead, recourse was had to epoxy resins for bonding the steel sheets to the plugs. It was found that, with care, the adhesives could withstand the static pressure differentials imposed on them when placed in the wind-tunnel wall. To obtain a good bond the surfaces are completely degreased by immersion in a 10% solution of sodium metasilicate for a period of 10 minutes. The brightness of the surfaces is then enhanced by immersing in an 85% phosphoric acid solution for 2 minutes.

Whilst the epoxy resin is setting, the plug and steel sheet are held together in a jig so that the panel remains flat. This clamping, which was not used when assembling the first 0.005" panel, does not cause panel tensioning and the jig is removed when the resin has hardened. To avoid

differential thermal expansion between the plug and panel due to localised heating, the resin is cured under normal room temperature. This does however have the disadvantage of increasing the curing time and slightly decreasing the strength of the bond.

The construction of a typical panel is shown in Fig. 14. The two clamping strips, along sections of the plug perimeter, are positioned after the resin has set and hence do not tension the panel. Their purpose is purely precautionary and is to prevent the panel from being carried into the tunnel in the event of a failure of the adhesive during tunnel operation. The region around the clamping strips is built-up with resin to present a surface which is flush with the tunnel wall.

4.4 Normal Modes

The normal modes of the panels are determined from panel response to discrete frequency excitation. The natural frequencies are obtained from measurements of amplitude and phase (relative to the exciting force) of the panel vibrations and the mode shapes are observed visually when sand particles are spread over the panel surface.

The frequencies of the low order modes were investigated, using electromagnetic excitation, for the 0.005" panel made first. The values obtained were found to be considerably higher than those estimated theoretically (Status Report No. 8). In particular, the measured fundamental frequency was in the range 160 c.p.s. to 260 c.p.s. (subject to positioning of equipment as discussed below) whilst the calculated value was 141 c.p.s.

It is believed that the discrepancy is due to the fact that the panel, when assembled, is not flat but has an appreciable curvature. This bow is very difficult to control but a satisfactory degree of flatness can probably

be achieved by the modified method of construction described in Section 4.3. Some approximate calculations based on comparisons between the natural frequencies of spherical caps as derived by Reissner in Reference 11 and those for flat circular plates (Reference 12) indicate that the degree of bowing to be expected can have an effect on the panel of similar magnitude to that measured above. As the natural frequencies of flat square plates of side a, and flat circular plates of diameter a differ by less than 3%, it is reasonable here to take the results for circular plates and apply them directly to square ones.

Closer examination of the measurements showed that the "apparent natural frequencies" depended markedly on the relative positions of the exciter, panel and proximity transducer used to measure the vibrations. This was most critical when exciter and transducer were both at the panel centre and, for these conditions, the observed variation of panel "fundamental" frequency with distance of transducer from panel is shown in Fig. 15. Unfortunately, before this phenomenon could be fully explored, the panel was damaged and had to be replaced. The investigation will, however, continue on the second panel using electromagnetic and acoustic excitation - the latter being of use only for modes for which the generalised force is non-zero.

4.5 Boundary Layer Excitation

The panel is mounted in the side wall of the 9" x 6" induced flow wind tunnel. The static pressure in the tunnel working section is below atmospheric and in the sub-sonic section the pressure differential is 2.3 to 2.4 p.s.i., dependong on position; this has a marked effect on the vibration of the thin panels placed in the tunnel wall.

The displacement power spectrum for the first 0.005" panel under a

pressure differential of 2.34 p.s.i. was shown in Fig.2 of Status Report No. 8. The main purpose of these measurements was, however, a comparison of the amplitudes of the panel vibration and the background vibration of the traverse gear and wind tunnel. It was found that the latter vibration was at least 20 db below the former throughout the spectrum and would therefore not influence measurements of panel vibration.

The outer face of the panel has now been enclosed by a sealed box in which the static pressure can be reduced to that of the tunnel. The background vibration is till of the same order of magnitude as previously measured but the overall panel vibration amplitude has increased by a factor of about 4. Panel displacement spectra have been measured at several positions on the surface of a second 0.005" panel and results for three of these positions are shown in Fig. 16. The pressure differential across the panel during the vibration measurements was 0.003 p.s.i.

The spectra show the presence of several panel normal modes and are in this respect considerably different in character from those previously measured under a greater pressure differential. Fig. 16 clearly shows the variation of the relative magnitude of the response in each mode with variation of position on the surface (i.e. as the vibration pick-up changes position in relation to the modes and antimodes of the mode), for example, the peak at 790 c.p.s. (Fig. 16 (a)) is barely discernible in Fig. 16(b) but has returned again in Fig. 16(c).

The natural frequencies of this panel have not yet been determined experimentally and hence the particular modes present in the above spectra cannot yet be identified. The frequency of the predominant peak (295 c.p.s.) does not however correspond with the calculated fundamental frequency (141 c.p.s.) of the panel.

5. Sound Radiation from a Turbulent Boundary Layer on a Rigid Surface

On the basis of the correlation pattern given by Equations (2.4) to (2.6) the acoustic power output from unit area of a (large) surface subject to turbulent boundary layer flow was found to be given by[2]

$$\frac{W}{(\rho_\infty U_\infty^{\,6} S/a_\infty^{\,3})} = 2.10^{-4} \left(\frac{p'}{q_\infty} \right)^2 \qquad \ldots(5.1)$$

REFERENCES

1. Bull, M.K. — "Instrumentation for and Preliminary Measurements of Space-Time Correlations and Convection Velocities of the Pressure Field of a Turbulent Boundary Layer" University of Southampton Report A.A.S.U. 149, August 1960.

2. Bull, M.K. Willis, J.L. — "Some Results of Experimental Investigations of the surface Pressure Field due to a Turbulent Boundary Layer" University of Southampton Report A.A.S.U. 199, November 1961. ASD-TDR-62-425

3. Bull, M.K. — "Space-Time Correlations of the Boundary Layer Pressure Field in Narrow Frequency Bands" University of Southampton Report A.A.S.U. 200, December 1961. ASD-TDR-62-722

4. Harrison, M. — "Pressure Fluctuations on the Wall Adjacent to a Turbulent Boundary Layer" David Taylor Model Basin Report 1260 December 1958.

5. Klebanoff, P.S. Tidstrom, K.D. Sargent, L.M. — "The Three-Dimensional Nature of Boundary Layer Instability" Jl. Fl. Mechs. Vol.12 1962.

6. Powell, A. — "On the Fatigue Failure of Structures due to Vibrations Excited by Random Pressure Fields" J.A.S.A. 30, p.1130, 1958.

7. Dyer, I. — "Sound Radiation into a Closed Space from Boundary Layer Turbulence" B.B.N. Report 602

8. Clarkson, B.L. Pietrusewicz, S.A. — "The University of Southampton Random Siren Facility" University of Southampton Report A.A.S.U. 204

9. Clarke, M.J. — "Response of a Rectangular Panel to Random Pressures" University of Southampton Report (to be published)

10.	Warburton, G.B.	"The Vibration of Rectangular Plates" Proc. I. Mech, E. 168, p.371, 1954.
11.	Reissner, F.	"On Vibrations of Shallow Spherical Shells" Jour. App. Phys. 17, p.1038, December, 1948.
12.	Morse, P.M.	"Vibration and Sound" (McGraw Hill) p.210.

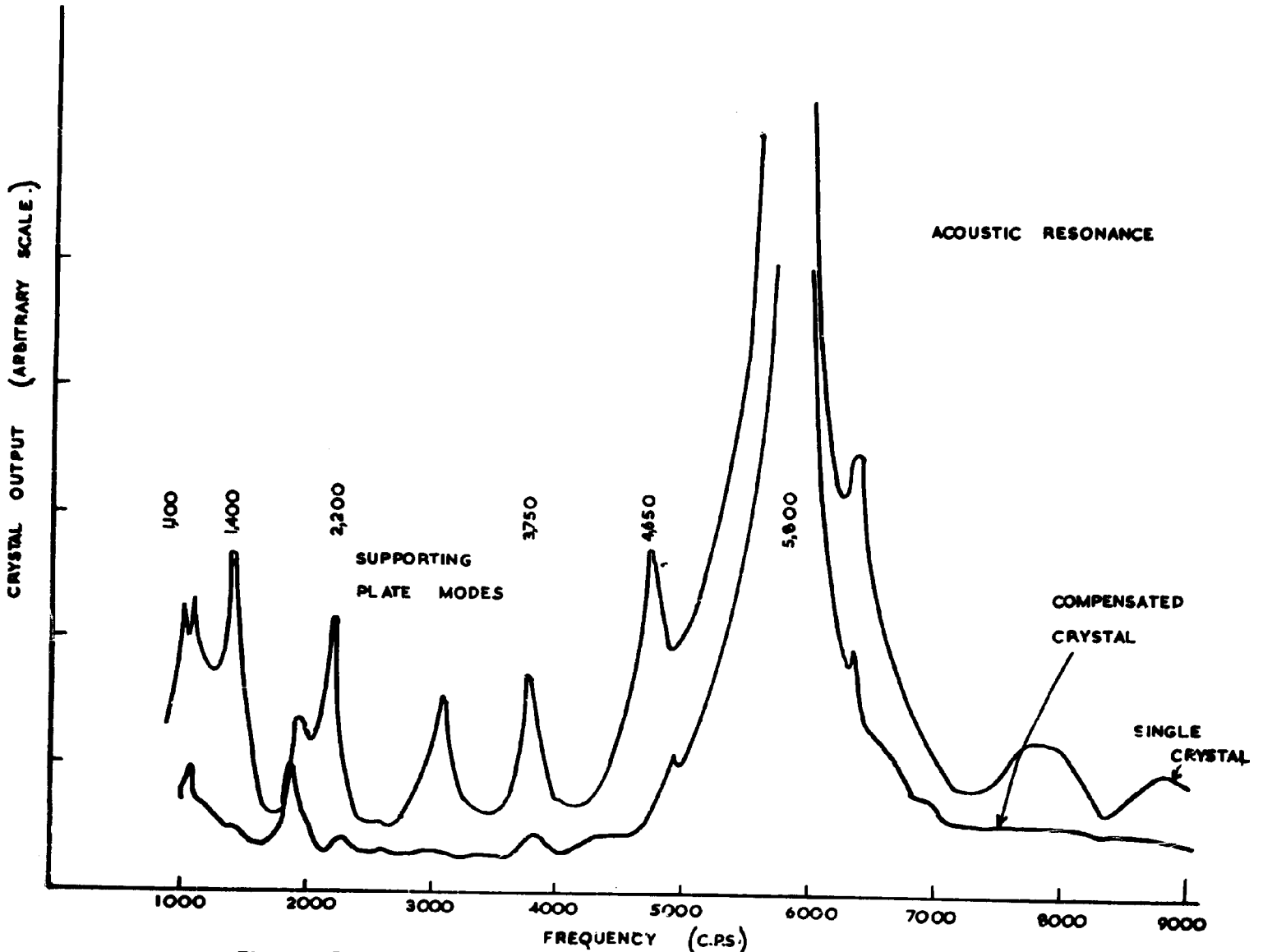

Figure 1. Effect of Crystal Compensation on Non-Isolated Transducer Mountings

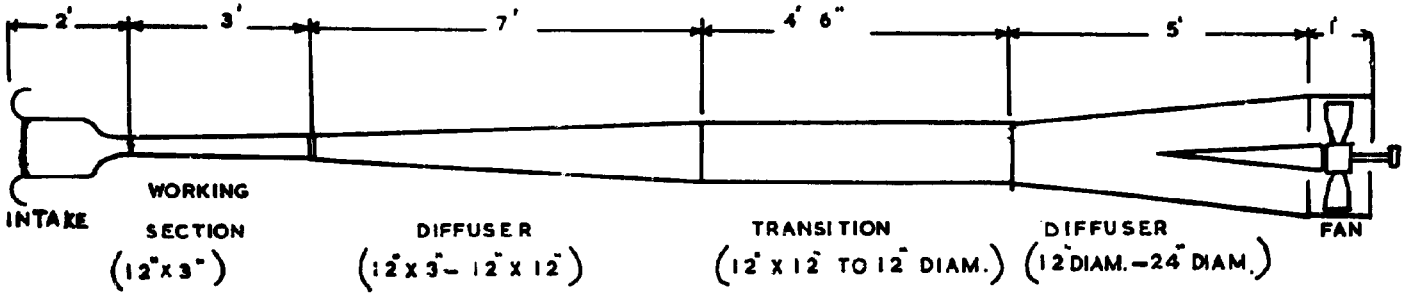

FIGURE 2 LOW SPEED BOUNDARY LAYER NOISE TUNNEL

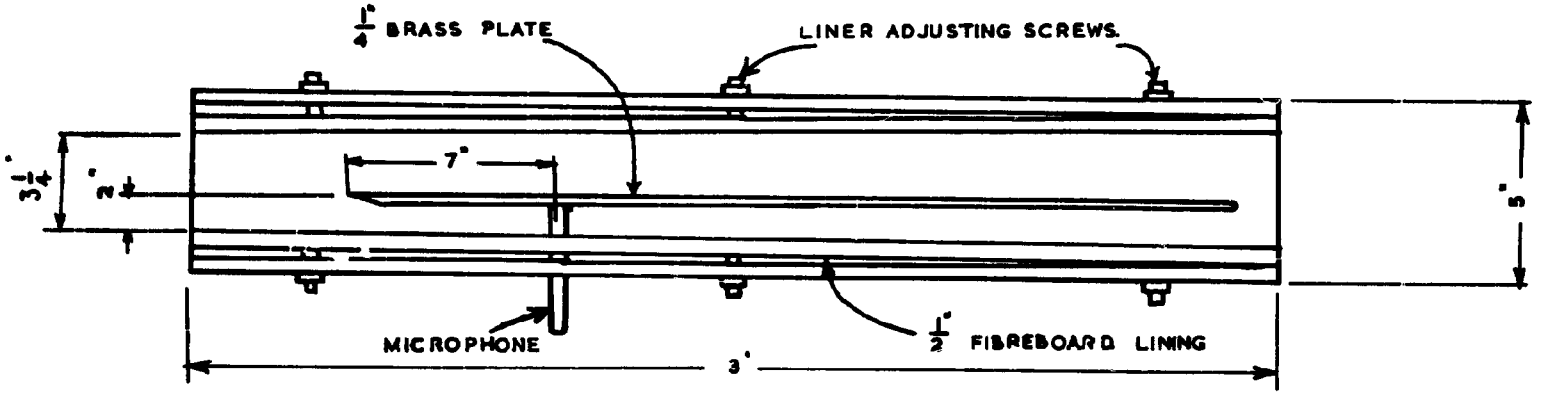

FIGURE 3 WORKING SECTION FOR LOW SPEED BOUNDARY LAYER NOISE TUNNEL

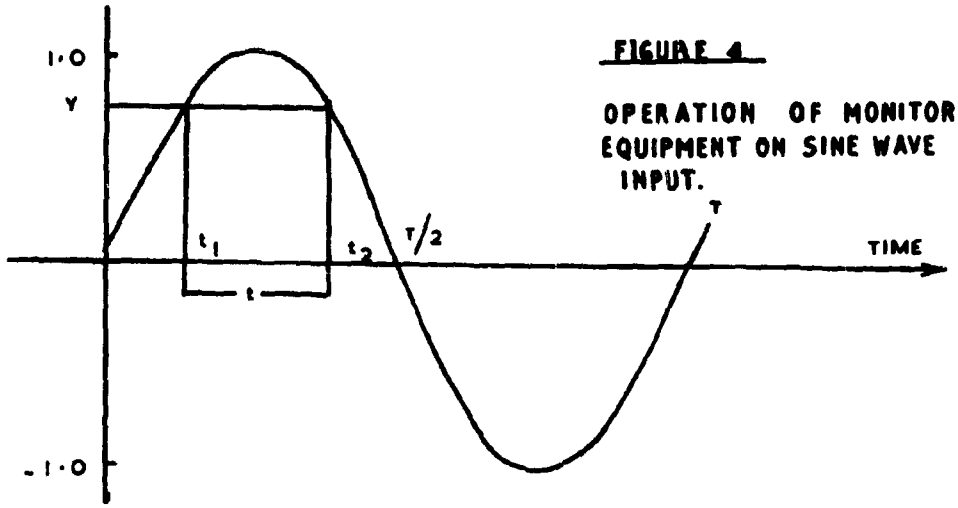

FIGURE 4

OPERATION OF MONITORING EQUIPMENT ON SINE WAVE INPUT.

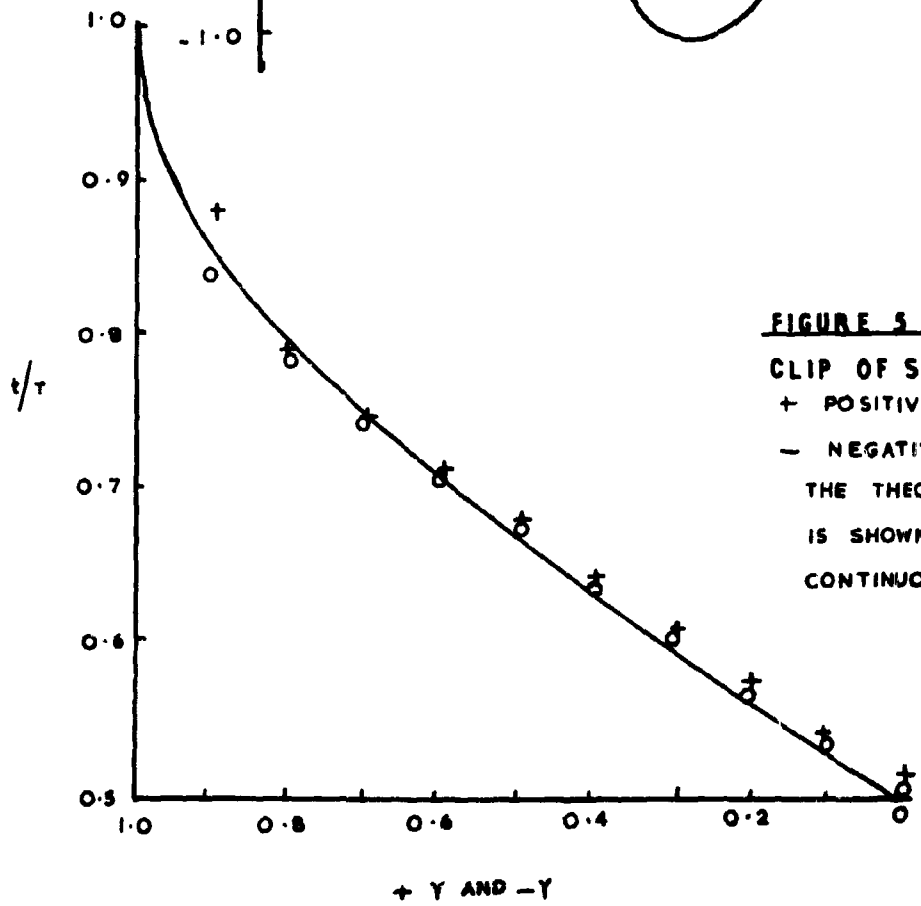

FIGURE 5

CLIP OF SINE WAVE.

\+ POSITIVE GOING

− NEGATIVE GOING

THE THEORETICAL RESULT IS SHOWN BY THE CONTINUOUS LINE.

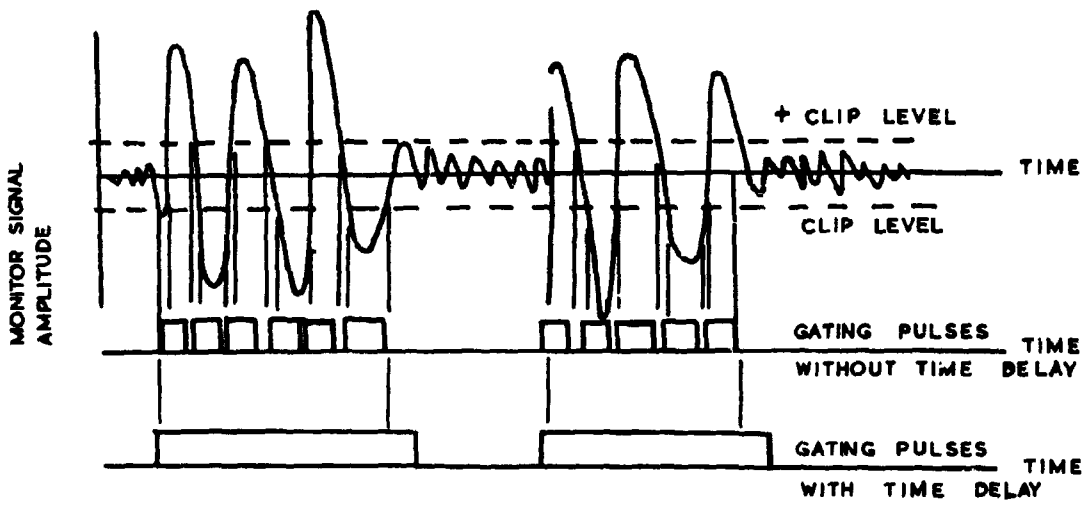

FIGURE 6 MONITORING OF INTERMITTENTLY TURBULENT SIGNALS

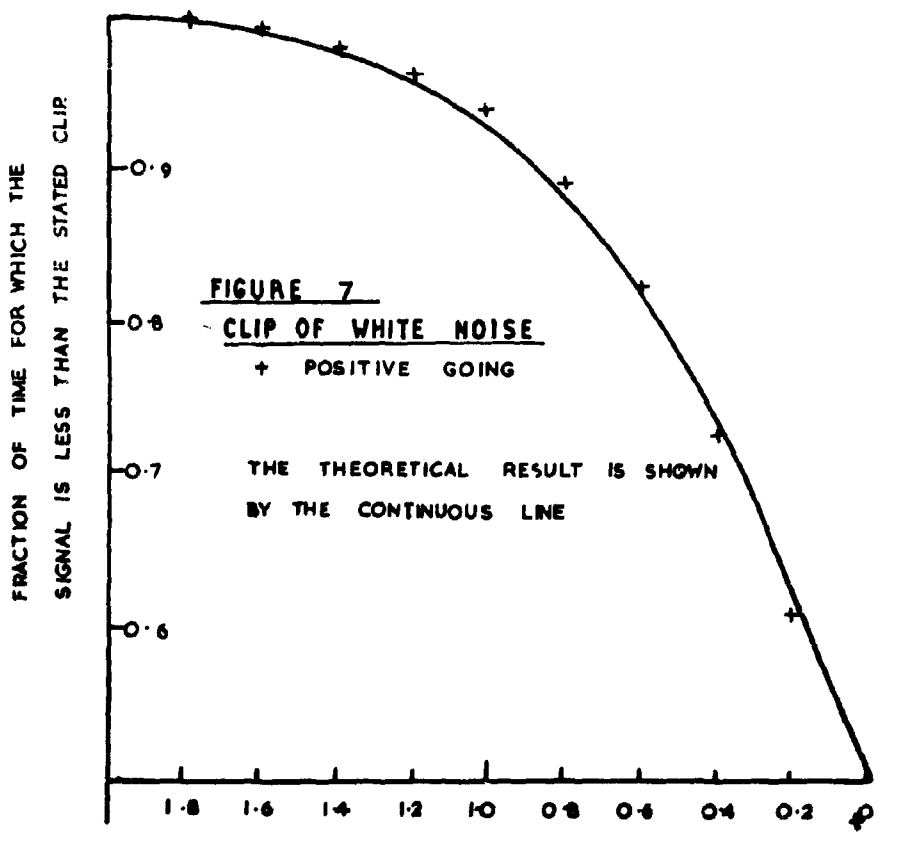

FIGURE 7
CLIP OF WHITE NOISE
+ POSITIVE GOING

THE THEORETICAL RESULT IS SHOWN BY THE CONTINUOUS LINE

Figure 7. CLIP AT STATED NUMBER OF STANDARD DEVIATIONS.

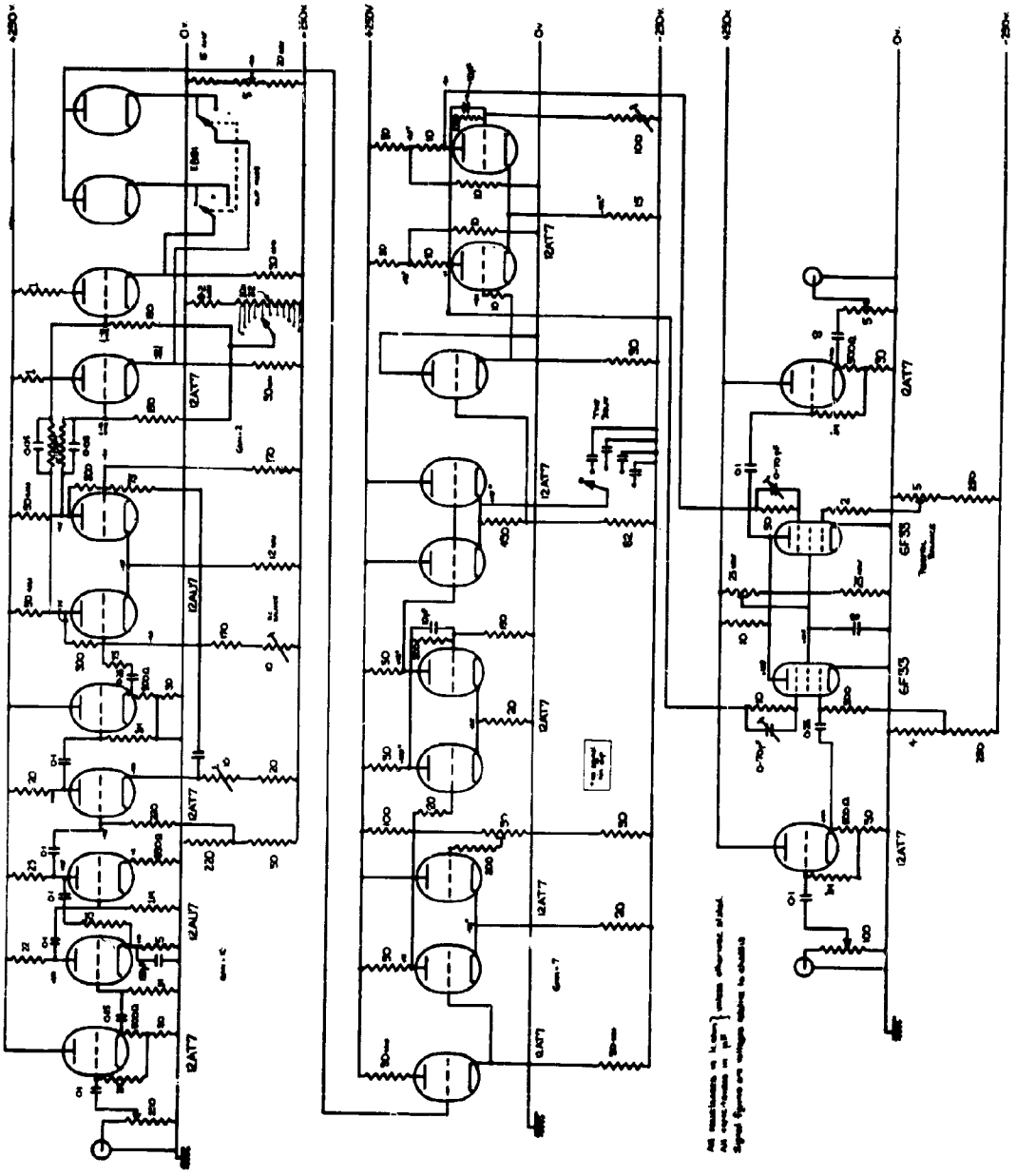

FIGURE 8: CIRCUIT DIAGRAM FOR TURBULENT MONITORING EQUIPMENT

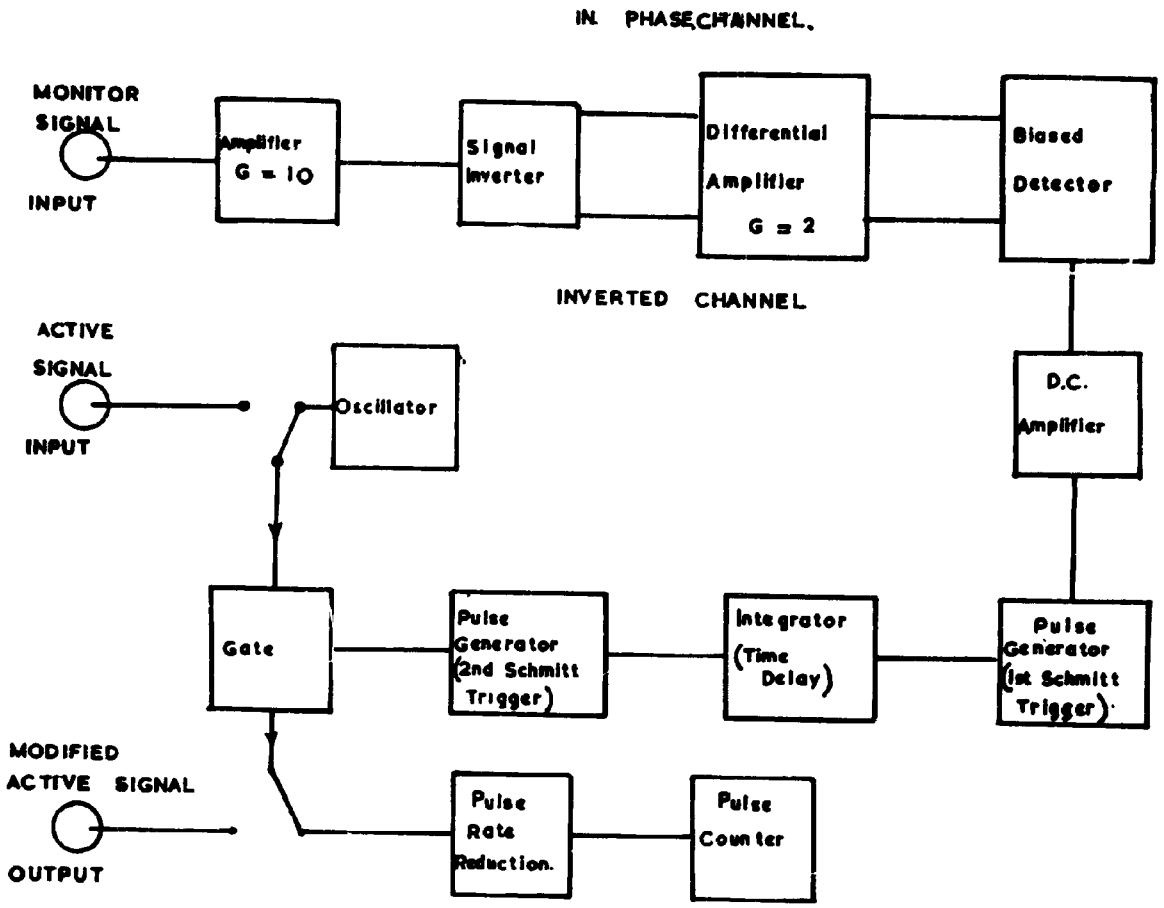

FIGURE 9 CIRCUIT BLOCK DIAGRAM FOR TURBULENCE MONITORING EQUIPMENT.

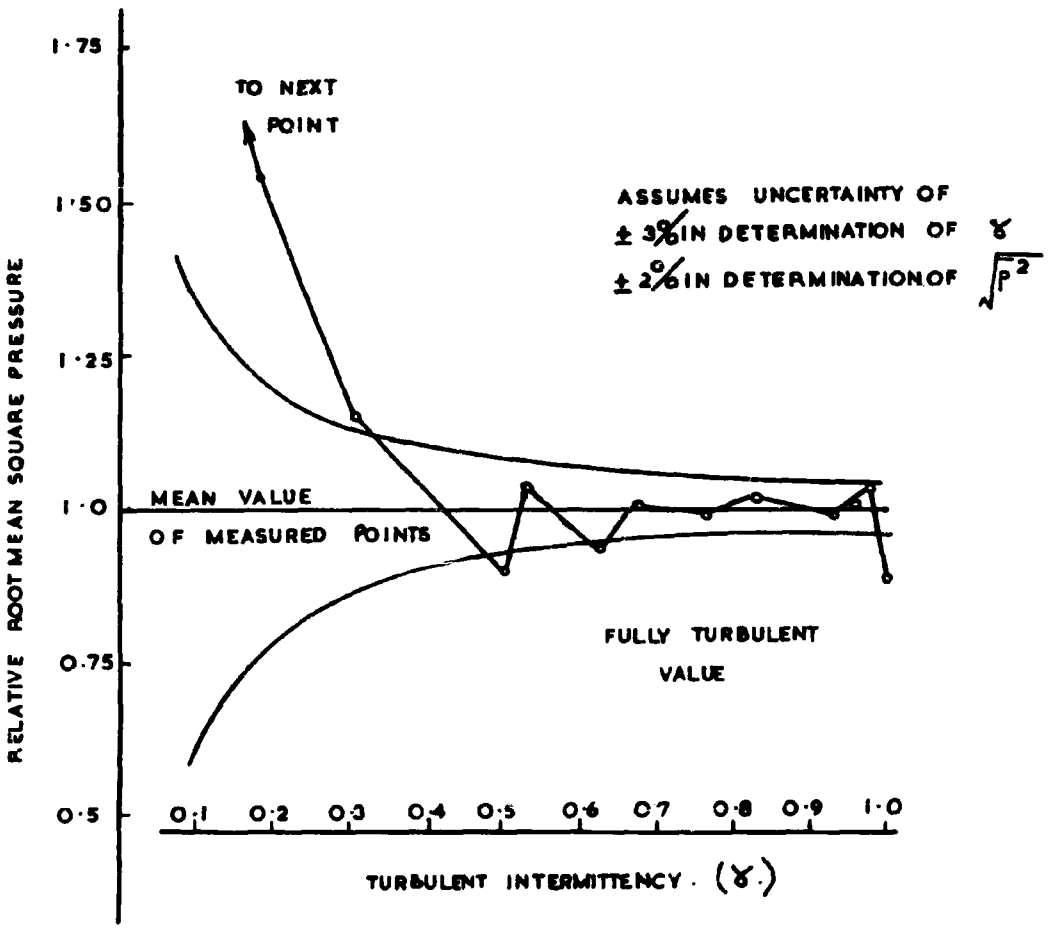

FIGURE 10 R.M.S. PRESSURE INSIDE TURBULENT SPOTS.

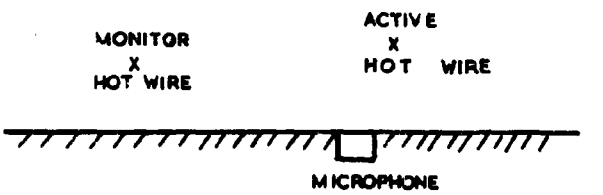

FIGURE 11. BASIC CONFIGURATION FOR MEASUREMENTS.

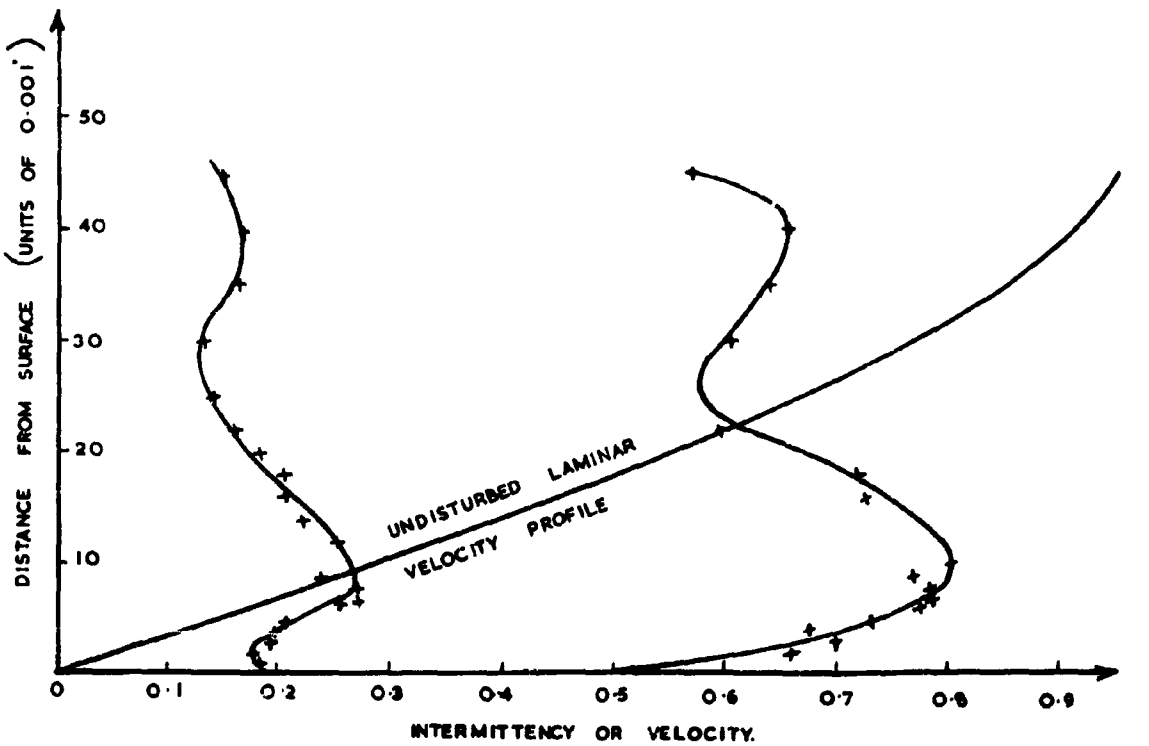

FIGURE 12. VARIATION OF INTERMITTENCY ACROSS BOUNDARY LAYER.

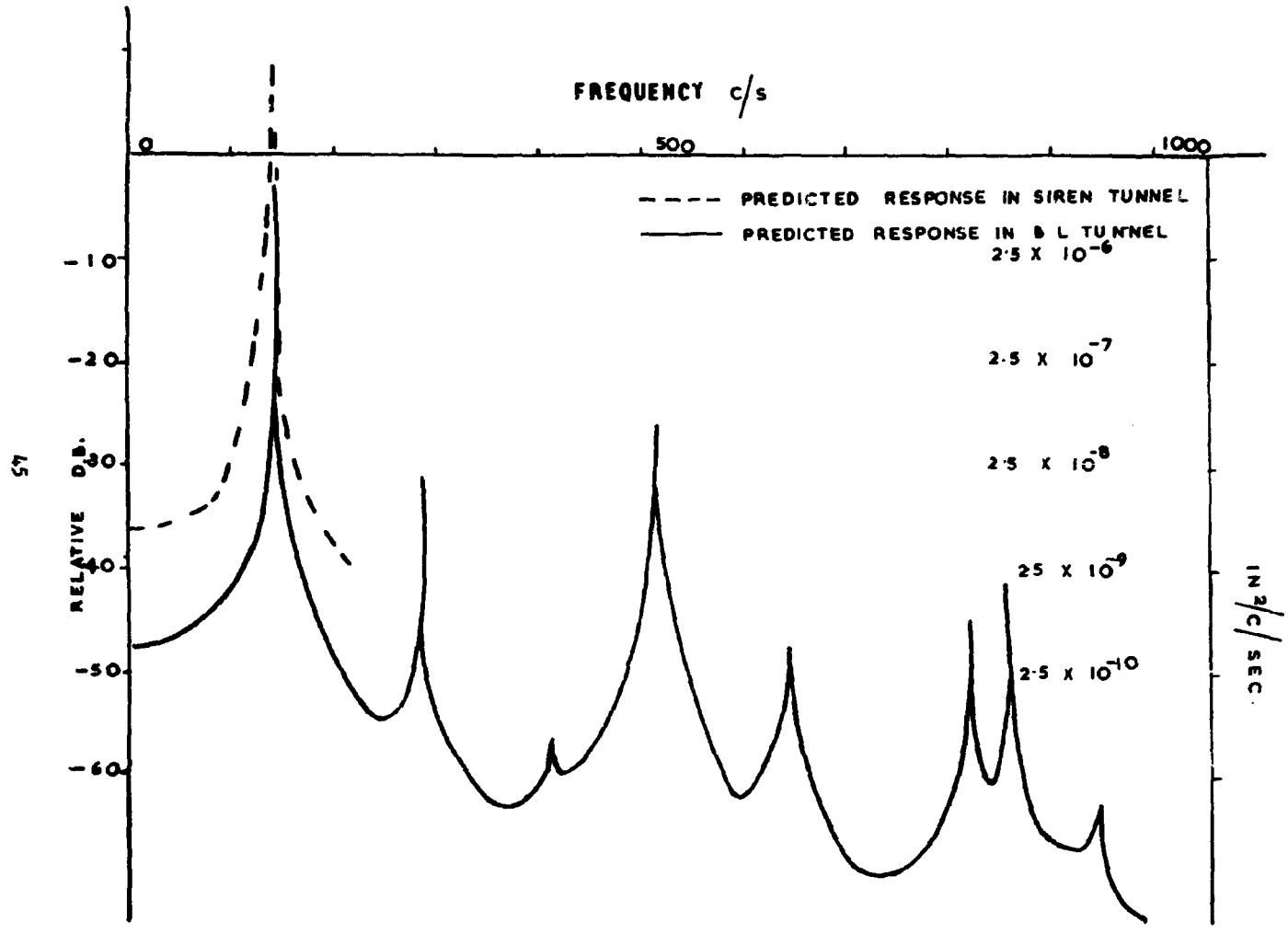

FIGURE. 13 PREDICTED POWER SPECTRAL DENSITY OF PANEL RESPONSE TO BOUNDARY LAYER EXCITATION. (0 - 1000 c/s)

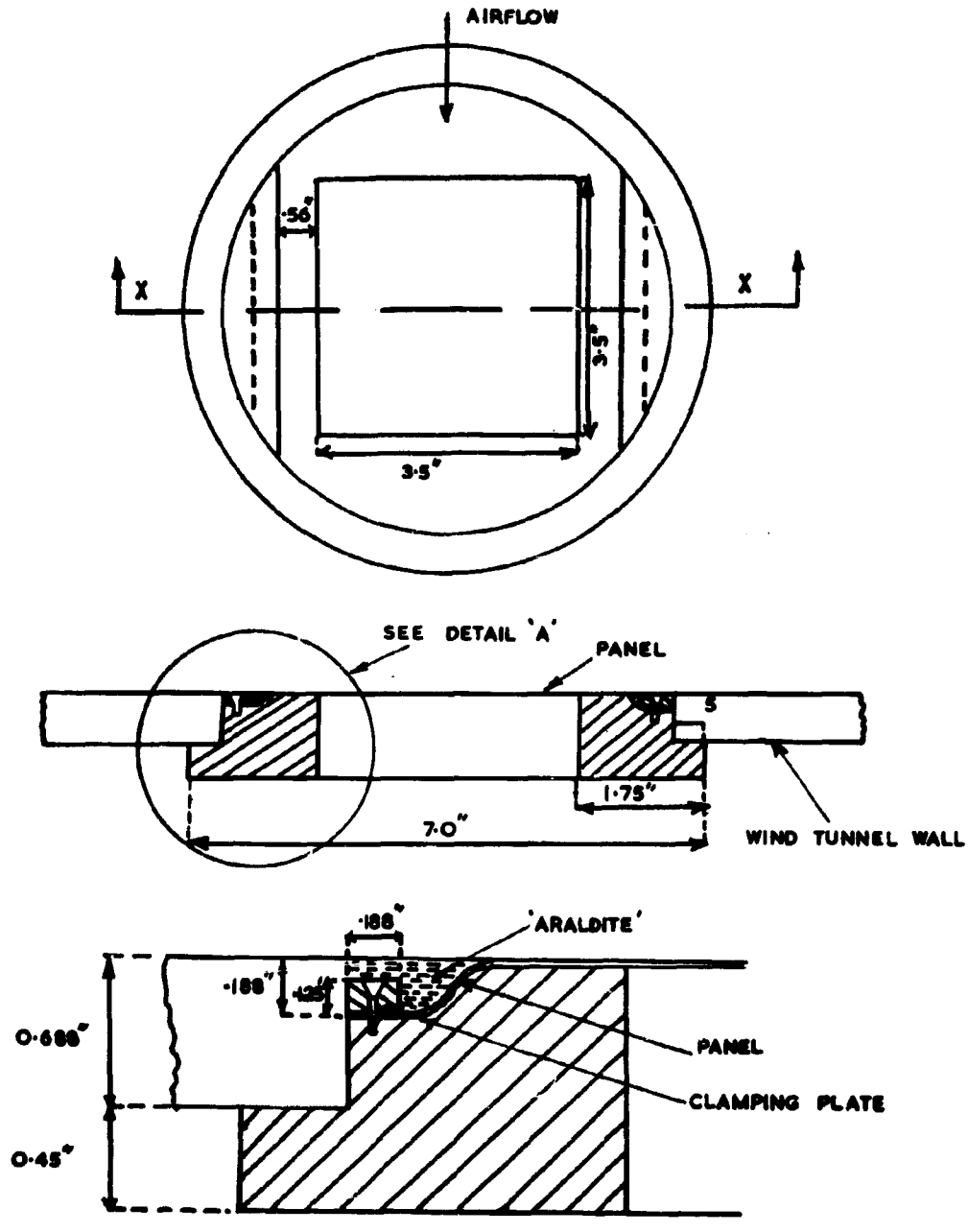

FIGURE 14 MOUNTING OF SQUAREPANEL FOR MEASUREMENT OF BOUNDARY LAYER EXCITED PANEL VIBRATIONS

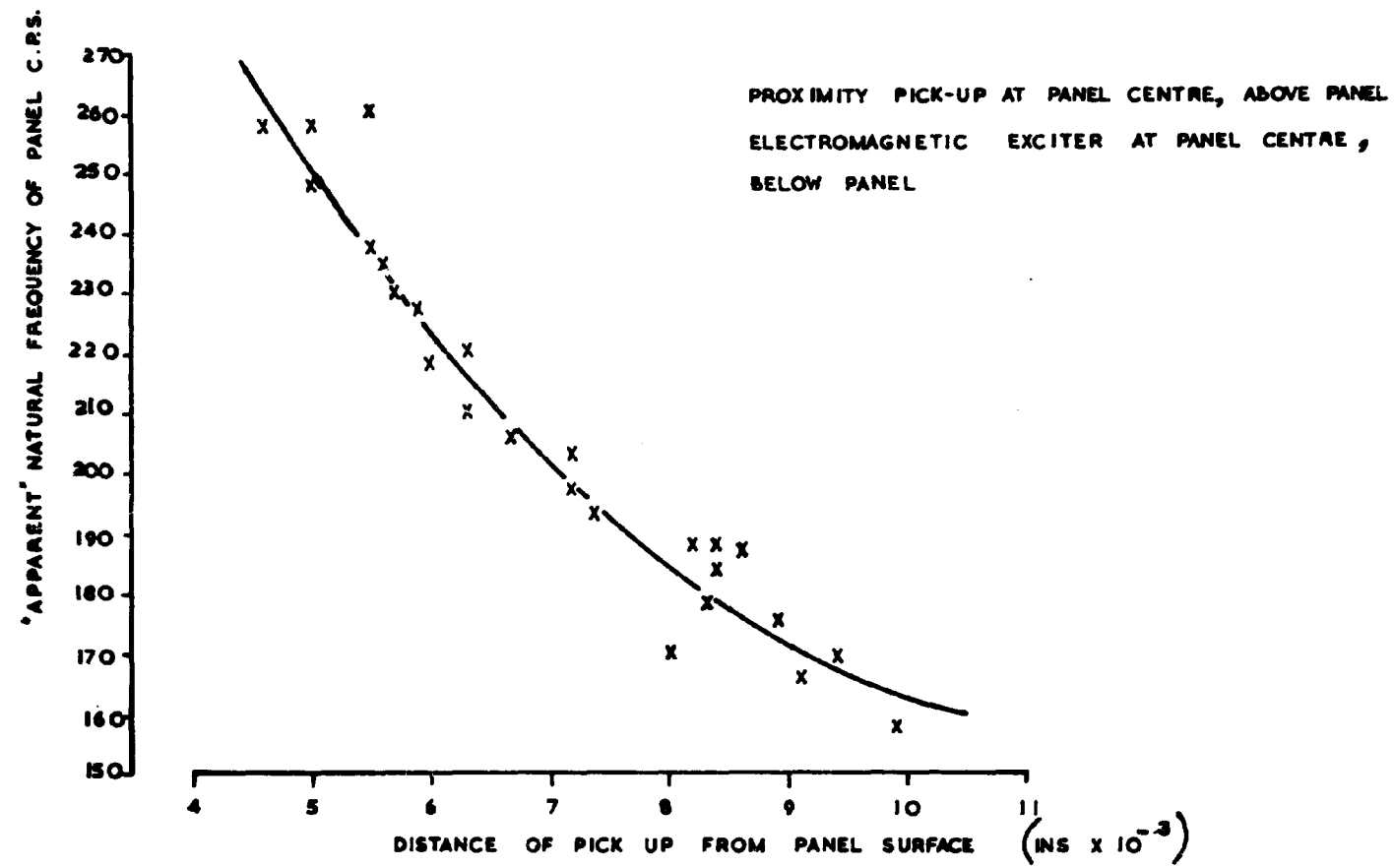

FIGURE 18 EFFECT OF DISTANCE OF PROXIMITY PICK-UP FROM SURFACE ON NATURAL FREQUENCY OF PANEL EXCITED ELECTROMAGNETICALLY.

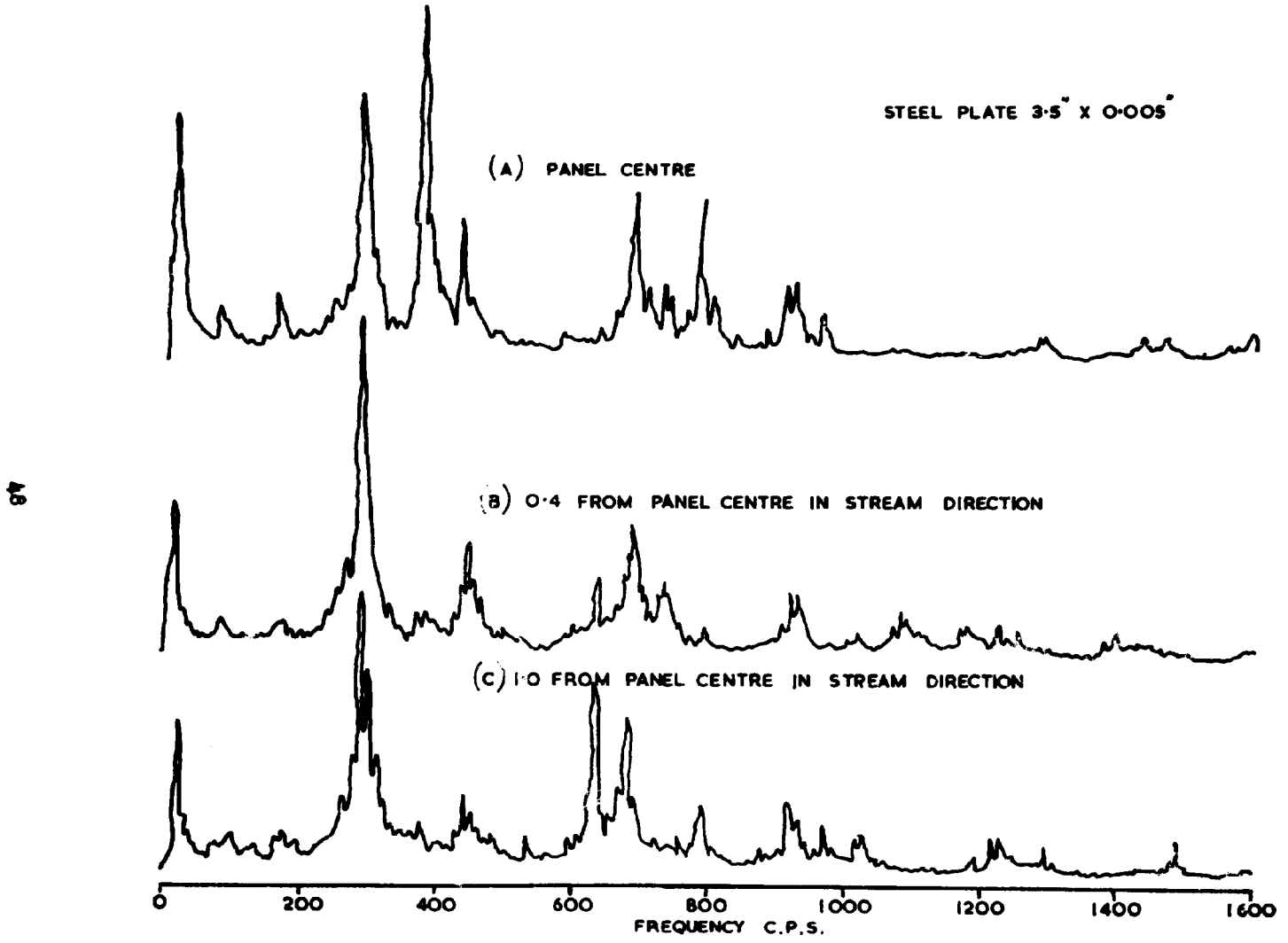

Figure 16. Displacement Spectra for Panel Excited by Boundary Layer Noise

UNCLASSIFIED